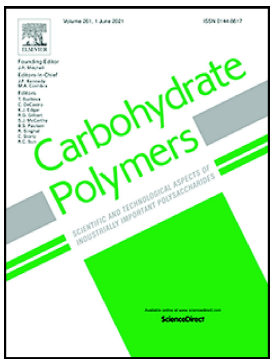

Thermomechanically processed chitosan:gelatin films being transparent, mechanically robust and less hygroscopic

Ying Chen, Qingfei Duan, Long Yu, Fengwei Xie

PII: S0144-8617(21)00909-7

DOI: https://doi.org/10.1016/j.carbpol.2021.118522

Reference: CARP 118522

To appear in: *Carbohydrate Polymers*

Received date: 16 June 2021

Revised date: 24 July 2021

Accepted date: 1 August 2021

Please cite this article as: Y. Chen, Q. Duan, L. Yu, et al., Thermomechanically processed chitosan:gelatin films being transparent, mechanically robust and less hygroscopic, *Carbohydrate Polymers* (2021), https://doi.org/10.1016/j.carbpol.2021.118522

Thermomechanically processed chitosan:gelatin films being transparent, mechanically robust and less hygroscopic

Ying Chen [a,b,1], Qingfei Duan [a,1], Long Yu [a], Fengwei Xie [c,] *

[a] *Collage of Food Science and Engineering, South China University of Technology, Guangzhou 510640, China*

[b] *Department of Food Science and Technology, National University of Singapore, Science Drive 2, 117542, Singapore*

[c] *International Institute for Nanocomposites Manufacturing (IINM), WMG, University of Warwick, Coventry CV4 7AL, United Kingdom*

*Corresponding author. Email: d.xie.2@warwick.ac.uk; fwhsieh@gmail.com (F. Xie)

[1] These authors contributed equally to this work.

Abbreviations: RH, relative humidity; TGA, thermogravimetric analysis; *WI*, whitish index; SEM, scanning electron microscopy; FTIR, Fourier-transform infrared; XRD, X-ray diffraction; DMTA, dynamic mechanical thermal analysis; WCA, water contact angle.

Abstract

Chitosan and gelatin are attractive polymeric feedstocks for developing environmentally benign, bio-safe, and functional materials. However, cost-effective methods to achieve advantageous materials properties and tailor their functionality are still lacking, but interesting. Herein, we found that physically mixing chitosan and gelatin at 1:1 (w/w) ratio resulted in materials with properties (higher Young's modulus (603.8 MPa) and tensile strength (33.6 MPa), and reduced water uptake (45%) after 6 h of water soaking) better than those of the materials based on mainly chitosan or gelatin. We attribute this synergy to the ionic and hydrogen-bonding interactions between the two biopolymers enabled by high-viscosity thermomechanical processing. Despite the lowest hygroscopicity, the 1:1 chitosan:gelatin films displayed the highest surface hydrophilicity. Besides, addition of gelatin to chitosan led to films being brighter, more transparent and amorphous. Thus, this work has generated new understanding to enhance the application of biopolymers for e.g. packaging, coating, and biomedical applications.

Keywords

Chitosan; gelatin; biopolymer composite; optical properties; mechanical properties; water absorption

Chemical compounds studied in this article

Chitosan (PubChem CID: 71853); Gelatin (PubChem CID: 381623137); Water (PubChem CID: 962); Glycerol (PubChem CID: 753); Acetic acid (PubChem CID: 176)

1 Introduction

Chitosan, a multifunctional polysaccharide formed by β-(1,4)-linked *N*-acetyl-D-glucosamine and D-glucosamine units, has some promising features from the application point of view, such as edibility, biodegradability, antimicrobial activity (Zhao, Wei, Xu, & Han, 2020), and biocompatibility (Pereda, Ponce, Marcovich, Ruseckaite, & Martucci, 2011). Therefore, chitosan has been widely explored as vaccine adjuvants (Li et al., 2021), dyes or heavy metal ion adsorbents (Aramesh, Bagheri, & Bilal, 2021; Zhang et al., 2021), drug delivery carriers (Kurakula, Gorityala, & Moharir, 2021), tissue engineering candidates (Wu, Dong, Li, Wang, & Cao, 2017), wound healers (Torkaman, Rahmani, Ashori, & Najafi, 2021), and disposable packaging materials (Wang, Ding, Ma, & Zhang, 2021). However, for high-volume applications such as environmental remediation and disposable packaging, chitosan is much more expensive and has less satisfactory material properties (weak mechanical properties and high hydrophilicity) than petroleum-derived plastics (Xu, Wei, Jia, & Song, 2020). Moreover, the transparency of the chitosan film is relatively low (Meng, Xie, Zhang, Wang, & Yu, 2018), which may also restrict its application.

Gelatin, obtained from partial hydrolysis of collagen, is one of the most widely used proteins in food (Alexandre, Lourenço, Bittante, Moraes, & Sobral, 2016; Zhang, Liang, Li, & Kang, 2020). Gelatin has advantages such as biodegradability, non-toxicity, biocompatibility, good film-forming ability and barrier properties, along with low cost (about 1/15 that of chitosan) (Ji et al., 2020). Gelatin has also been used in food packaging (Nur Hanani, Roos, & Kerry, 2014; Roy & Rhim, 2020), controlled drug release (An, Gou, Yang, Hu, & Wang, 2013), biomedical (Yang, Li, & Nie, 2007), and battery (Sun et al., 2008) applications. However, the application of gelatin may be

hindered by its high hygroscopicity, low thermal stability, and relatively poor mechanical properties (brittleness) (Ebrahimi, Fathi, & Kadivar, 2019; Guo et al., 2013).

Polymer blending can result in improvement in the physical properties of individual components (Meng et al., 2018). Interactions between different polymers may lead to improved mechanical properties (Pereda et al., 2011). Thus, the mixing of gelatin and chitosan could be a promising way to obtain new materials with enhanced physicochemical properties and new functionality. Charged carboxylic groups (COO─) from gelatin amino acids can electrostatically interact with the protonated amino groups of chitosan, resulting in stable polyelectrolytic complexes and transparent and homogeneous films (Qiao, Ma, Zhang, & Yao, 2017; Rivero, García, & Pinotti, 2009; Rodrigues, Bertolo, Marangon, Martins, & Plepis, 2020).

Researchers characterized the molecular interactions in chitosan–collagen complexes by viscometry, wide-angle X-ray scattering (WAXS), and Fourier-transform infrared (FTIR) spectroscopy. It was found that chitosan and collagen can interact with each other at the molecular level (Qiao et al., 2017; Sionkowska, Wisniewskia, Skopinskaa, Kennedy, & Wess, 2004). Furthermore, it was found that a polyelectrolyte complex could be formed with pH > 4.7 (pH_{iso} of gelatin) in a chitosan–gelatin solution (Yin, Li, Sun, & Yao, 2005). Then, the composite films prepared from gelatin (or collagen) and chitosan have been found to possess improved antimicrobial activity, mechanical or barrier properties compared with those of the single-component films (Pereda et al., 2011; Rivero et al., 2009).

While solution methods have been widely used in research studies for preparing biopolymer materials (e.g. films, hydrogels, and nanofibers) (Astaneh et al., 2020; Chiono et al., 2008; Ebrahimi

et al., 2019; Pereda et al., 2011; Qiao et al., 2017; Wang et al., 2021; Wu et al., 2017; Yin et al., 2005), they may suffer from the drawbacks of low efficiency and high solvent waste generation. Thermoplastic methods are more feasible to produce films on an industrial scale, which is less solvent-demanding and can provide high shear forces and processing temperature (Wang et al., 2021). Moreover, material mixing and molecular interactions might occur in different ways under high-viscosity conditions, which has been studied to a very limited extent. It was recently reported that thermomechanical processing could lead to chitosan:silk peptide and chitosan:carboxymethyl cellulose materials with unexpected mechanical properties (Meng et al., 2018) and hydrolytic stability (Chen, Xie, Tang, & McNally, 2020a), respectively. In this regard, high-viscosity mixing of polyelectrolyte biopolymers could lead to better ionic and hydrogen-bonding interactions between biopolymer chains (Chen et al., 2020a; Meng et al., 2018). However, to the best of our knowledge, there has been no study hereto on chitosan:gelatin hybrid materials obtained by thermomechanical processing.

This work is based on the hypothesis that molecular interactions between chitosan and gelatin, if properly realized, can lead to chitosan:gelatin materials with better properties than those of materials based on primarily chitosan or gelatin. Glycerol is one of the most widely used plasticizers for biopolymers due to its non-volatility, large availability, matching hydrophilicity, and low exudation (Chen et al., 2020a; Epure, Griffon, Pollet, & Avérous, 2011). In this work, we prepared chitosan:gelatin composite films with limited amounts of solvents using thermomechanical mixing and compression molding. The molecular interactions between gelatin and chitosan and the morphology, structure, and physical properties (mechanical properties, thermal stability, glass

transition temperature, and water absorption) of the composite films were investigated. In particular, we found blending a certain content of gelatin into chitosan is instrumental to the processing of chitosan and to achieving advantageous material properties. Thus, this work could be insightful for the development of cost-effective high-performance biopolymer materials.

2 Experimental

2.1 Materials

Chitosan (CS), derived from crustaceous shells, with a specification of BR, was purchased from Jinan Xinhong Huagong Co., Ltd (Jinan, China). This chitosan has a degree of deacetylation (DD) of 90% and a viscosity of about 400 mPa·s (1% solution in 1% acetic acid at 25 °C). It had an original moisture content of 10.65 wt% measured by weight loss during drying. Gelatin (GA), in food-grade (type A, bloom index 250), was supplied by Rousselot Gelatin Co., Ltd (Wenzhou, China). The original moisture content of the gelatin is 13.10 wt%. Glycerol (AR grade) and acetic acid (AR grade) were purchased from Sinopharm Chemical Reagent Co., Ltd (Shanghai, China). All these chemicals were used as received without further purification.

2.2 Sample preparation

Different samples were prepared according to the formulations listed in **Table 1**. The sample codes such as "75CS-7.5%" was used, where "75CS" represents the mass percentages of dry chitosan in the biopolymer matrix while "7.5%" indicates the mass content of glycerol added to the biopolymer matrix. Chitosan and gelatin were mixed by mechanical stirring for 10 min, during which 2 M acetic acid and glycerol were added dropwise. The mixtures were stored overnight at 4 °C. For each batch, 80 g of the mixed sample was thermally kneaded (80 rpm screw speed, 80 °C) for 15 min

using a twin-rotor HAAKE Rheomix mixer coupled with a Polylab RC600p system (ThermoHaake, Germany). Afterward, 35 g of the thermomechanically processed material was hot-pressed (80 °C, 2500 psi, 10 min) into a film using a flat sulfaration machine (Guangzhou Shunchuang Rubber Machinery Company, Guangzhou, China) along with a mold with a 100 mm × 100 mm × 1 mm hollow molding space. The hot-pressed films were soaked in methanol for 12 h and then washed with distilled water. All the specimens were dried in an oven at 30 °C for 24 h and then stored in a desiccator (57% relative humidity (RH)) for 4 weeks, followed by conditioning at either 57% RH or 75% RH for another week before characterization. Except for thermogravimetric analysis (TGA) and mechanical testing, structure and property analyses were performed for the samples conditioned at 57% RH only.

Table 1 Sample codes and formulations.

Sample	Gelatin dry mass (g) [a]	Chitosan dry mass (g) [a]	Glycerol (g) [a]	2 M Acetic acid (mL)
100CS	–	26 (100%)	–	61.90
100CS-7.5%	–	26 (100%)	1.95 (7.5%)	59.95
100CS-15%	–	26 (100%)	3.90 (15%)	58.00
75CS	6.5 (25%)	19.5 (75%)	–	61.69
75CS-7.5%	6.5 (25%)	19.5 (75%)	1.95 (7.5%)	59.74
75CS-15%	6.5 (25%)	19.5 (75%)	3.90 (15%)	57.79
50CS	13 (50%)	13 (50%)	–	61.49
50CS-7.5%	13 (50%)	13 (50%)	1.95 (7.5%)	59.54
50CS-15%	13 (50%)	13(50%)	3.75 (15%)	57.59
25CS	19.5 (75%)	6.5 (25%)	–	61.29

25CS-7.5%	19.5 (75%)	6.5 (25%)	1.95 (7.5%)	59.34
25CS-15%	19.5 (75%)	6.5 (25%)	3.90 (15%)	57.39

[a] The numbers in the brackets are the mass percentages of either biopolymer or glycerol based on the total mass of the biopolymer matrix.

2.3 Characterization

2.3.1 Optical properties measurement

The color of the films was determined using a CIE colorimeter (X-Rite, Inc., USA). The *L* (lightness/brightness), *a** (redness/greenness) and *b** (yellowness/blueness) values were obtained by placing the film on a white reflector standard plate. Five measurements were taken on each film surface. Then, the total difference in color (ΔE) was calculated according to the equation as follow (Boekel, 1996):

$$\Delta E = \sqrt{(\Delta a)^2 + (\Delta b)^2 + (\Delta L)^2} \quad (1)$$

where ΔL, Δa, and Δb are the differences between the corresponding color parameters of the sample and that of the white standard (L = 93.63, a = 0.95, and b = 0.46).

Whitish index (*WI*) was calculated according to the equation as follow (Avena-Bustillos, Cisneros-Zevallos, Krochta, & Saltveit, 1994):

$$WI = 100 - ((100 - L)^2 + a^2 + b^2)^{1/2} \quad (2)$$

2.3.2 Transparency

A UV–visible spectrophotometer (Lambda 1050+, PerkinElmer, USA) was used to measure the light transmittance (T_{500}) of the films at a wavelength of 500 nm. The test was carried out in triplicate

for each sample.

2.3.3 Scanning electron microscopy (SEM)

The cryo-fractured surface morphologies of the biopolymer films were investigated using a scanning electron microscope (Phenom, Eindhoven, Netherlands) operated at a voltage of 10 kV. The samples were fractured with liquid nitrogen and were coated with gold for 90 s using a Q-150R-S sputter-coater (Quorum Technologies Ltd, UK) under vacuum before SEM imaging.

2.3.4 Fourier-Transform Infrared (FTIR) Spectroscopy

FTIR spectroscopy was performed using a PerkinElmer Frontier FTIR spectrometer (Spectrum-3, Germany) fitted with a Zn-Se attenuated total reflectance (ATR) accessory. FTIR spectra were collected against the air as the background over a wavenumber range of 4000–600 cm^{-1} at a resolution of 4 cm^{-1}. Each collection was based on 64 scans.

2.3.5 X-ray diffraction (XRD)

XRD analysis of the conditioned chitosan:gelatin films was performed using an Xpert PRO diffractometer (Bruker, Germany) at 40 mA and 40 kV with Cu Kα radiation (wavelength: 0.15418 nm) as the X-ray source. The scanning diffraction angle (2θ) was from 5° to 60° with a scanning speed of 2.16 s/step and a scanning step of 0.02°.

2.3.6 Dynamic mechanical thermal analysis (DMTA)

A PerkinElmer Pyris Diamond DMA8000 instrument was used to evaluate the dynamic mechanical properties of the films as rectangular tensile bars in the single cantilever tensile mode. The length of the tested tensile section was 20 mm. The tests were carried out at a frequency of 1 Hz and a strain of 0.05% with a heating ramp from −50 °C and 200 °C at 2 °C/min. The dynamic storage

modulus (E'), loss modulus (E''), and loss tangent (tan $\delta = E''/E'$) were obtained. To prevent water evaporation during the tests, the specimens were coated with silicone oil.

2.3.7 Thermogravimetric Analysis (TGA)

A PerkinElmer Diamond TGA STA 8000 facility was used to determine the thermal decomposition temperatures of the samples with a temperature ramp from 30°C to 700 °C at 10 °C/min in a nitrogen atmosphere. For each measurement, about 3 mg of the sample was weighed on a platinum pan.

2.3.8 Tensile testing

According to the ASTM D882-18 standard, the tensile mechanical properties of the biopolymer films were evaluated using a tensile testing apparatus (Instron ASTM D638) with a 100 N load cell at a cross-head speed of 5 mm min^{-1} at room temperature. For each sample, the data were generated based on seven specimens.

2.3.9 Water absorption

The water absorption of the biopolymer films was evaluated by measuring the weight percentages of the films at different time points after immersing in distilled water. Specifically, the film specimens (4 cm × 4 cm) were placed in a 500 mL beaker containing 300 mL of distilled water under ambient temperature (25 °C). The samples were then taken out at intervals, wiped with Whatman filter paper to remove the excess water on the surface, and weighed (with an accuracy of 0.01 g). The water absorption was expressed as:

$$\text{Water absorption}(\%) = \frac{M_t - M_0}{M_0} \times 100 \qquad (3)$$

where M_0 is the initial mass of the specimen before water soaking and M_t the mass of the specimen

after soaking in water for a certain time (t).

2.3.10 Contact angle test

The contact angle of water droplets (3 μL) on the films after 5 s and 60 s was measured using a contact angle system ZJ-7000 (Z. Jia Equipment, Shenzhen, China) at room temperature. For each sample, four different places were measured.

3 Results and Discussion

3.1 Appearance and optical parameters

Fig. S1a shows the different biopolymer films had different color shade and transparency. While the 100CS group of films were the darkest and most opaque, the composite films with a higher content of gelatin were brighter and more transparent. **Table 2** shows the L, a*, and b* values of the films. The 25CS-15% film showed the highest WI value and the lowest ΔE value while the 100CS group displayed the reverse. Besides, **Table 2** shows that the 100CS group of films had the lowest T_{500} values (2.14–3.99%) and the 25CS group had the highest (51.49–62.56%), which confirms the highest transparency of the latter. The differences in optical characteristics among the composite films can be attributed to the different colors of chitosan and gelatin after processing.

Table 2 Optical characteristic values of the different films.

Sample	L	a	b	ΔE	WI	T_{500}
100CS	41.21±0.22	21.59±0.28	36.05±0.21	67.68±0.32	27.73±0.14	3.99±0.04
100CS-7.5%	37.43±0.30	17.00±0.34	29.05±0.07	66.14±0.32	28.95±0.33	5.66±0.03
100CS-15%	45.82±0.13	15.82±0.11	41.26±0.52	65.74±0.45	30.08±0.43	2.14±0.04
75CS	50.97±0.26	11.35±0.25	46.30±0.26	64.51±0.40	31.61±0.40	13.08±0.03

75CS-7.5%	51.58±0.59	11.95±0.46	45.66±0.35	63.74±0.39	32.37±0.42	17.41±0.03
75CS-15%	56.71±0.15	13.08±0.10	44.56±0.39	59.77±0.50	36.53±0.50	12.4±0.01
50CS	53.40±0.36	8.18±0.53	42.48±0.22	59.67±0.19	36.41±0.06	21.07±0.02
50CS-7.5%	59.34±0.51	2.59±0.30	36.34±0.37	50.72±0.59	45.40±0.59	42.6±0.01
50CS-15%	60.26±0.32	0.58±0.07	32.61±0.48	47.42±0.43	48.59±0.41	41.69±0.03
25CS	64.89±0.12	−1.95±0.04	21.32±0.47	36.75±0.35	58.87±0.32	51.49±0.03
25CS-7.5%	64.93±0.63	−2.01±0.07	20.63±0.08	36.32±0.56	59.26±0.58	61.23±0.03
25CS-15%	65.88±0.17	−0.244±0.24	18.86±0.08	34.59±0.25	60.94±0.27	62.56±0.05

3.2 Morphology

Fig. 2 shows the SEM images of cryo-fractured surfaces of the different biopolymer films. While the 100CS film still contained raw chitosan particles, addition of glycerol, as a plasticizer, facilitated the processing of chitosan as shown by the more cohesive structure of 100CS-7.5% and 100CS-15%. All the chitosan:gelatin composite films displayed a cohesive structure irrespective of the presence of glycerol, which indicates that gelatin, with a low gel–sol transition temperature (around 40 °C), assisted the processing of chitosan by decreasing the overall viscosity. In this study, a film based on pure gelatin could not be obtained by thermomechanical processing as the pure gelatin became liquid due to its low gel–sol transition temperature. All the samples of different chitosan/gelatin ratios exhibited a homogenous structure without apparent phase separation, suggesting the excellent compatibility and strong interactions between the two biopolymers.

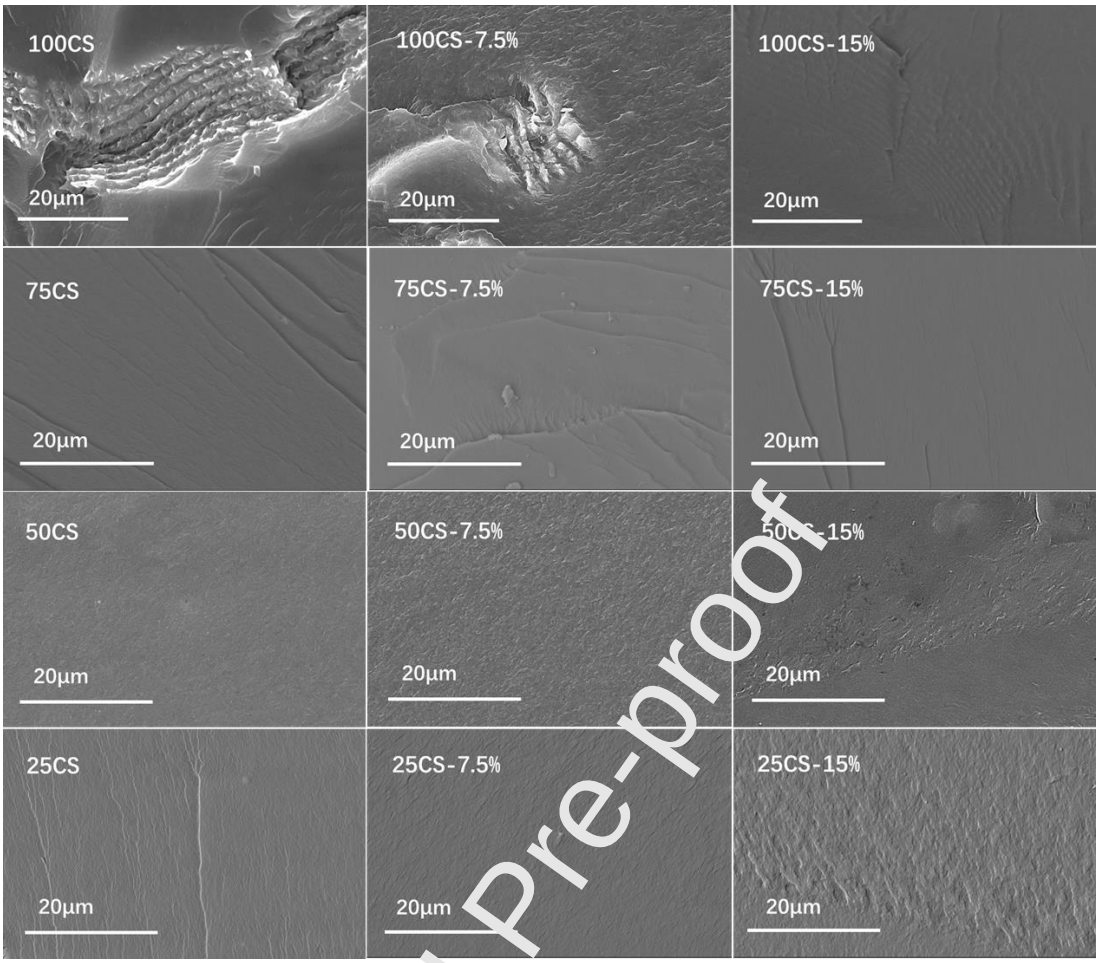

Fig. 1. SEM of cryo-fractured surfaces of the different chitosan:gelatin films.

3.3 Molecular interactions

FTIR analysis was conducted to understand the chemical interactions in the different chitosan:gelatin films (**Fig. 2**). In **Fig. 2**a, for raw gelatin, there were absorption bands at 2921 cm^{-1} (amide B: CH_2 asymmetric stretching), 1630 cm^{-1} (amide I: C═O stretching), 1526 cm^{-1} (amide II: 40% C─N and N─H vibration), and 1235 cm^{-1} (amide III: C─N and N─H vibrations and CH_2 groups) (Abuibaid, AlSenaani, Hamed, Kittiphattanabawon, & Maqsood, 2020; Chen et al., 2020a; Qiao et al., 2017). The broad peak at about 3291 cm^{-1} and the small peak at 1446 cm^{-1} are due to ─OH groups (Ebrahimi et al., 2019; Sionkowska et al., 2004). For chitosan, the absorption band of

the amino group in the region of 3292–3355 cm^{-1} was masked by the broad absorption band from ─OH groups (Sionkowska et al., 2004). The main characteristic absorption bands of chitosan at 1650 and 1259 cm^{-1} can be assigned to amide I and amide III, respectively. These amide bands suggest chitosan is only partially deacetylated (Sionkowska et al., 2004). The intense absorption bands at 1589 cm^{-1} are due to the amino group (Yin et al., 2005). The absorption bands at 1060, 991 and 894 cm^{-1} (C─N stretching) and 1024 cm^{-1} (C─O stretching vibration) are due to the carbohydrate ring skeleton (Kittur, Vishu Kumar, & Tharanathan, 2003; Lawrie et al., 2007).

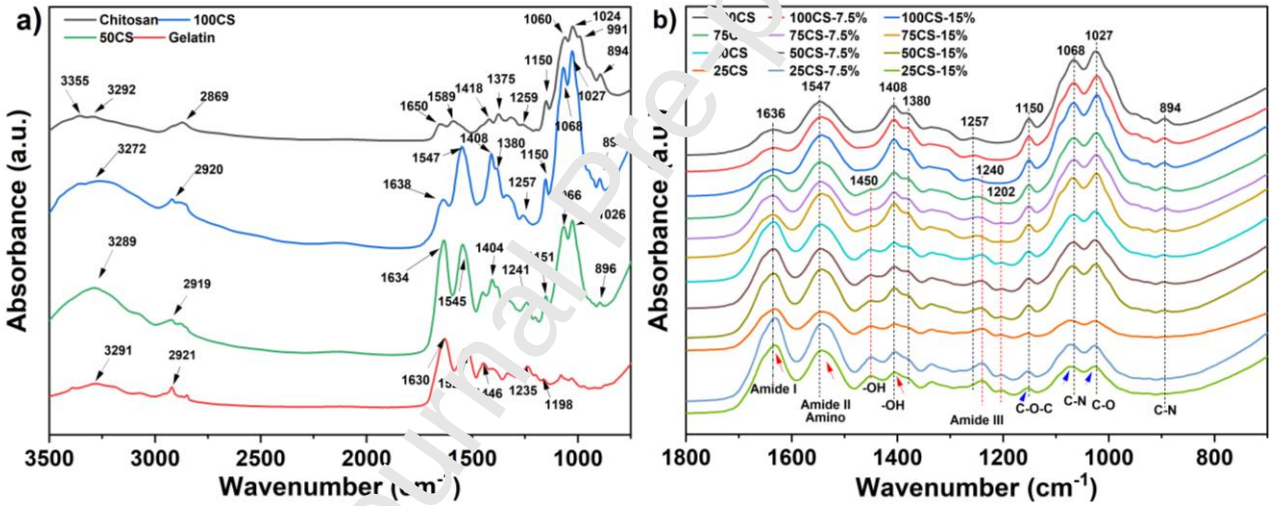

Fig. 2. FTIR spectra for raw chitosan, raw gelatin, and the different chitosan:gelatin films.

Table 3 FTIR bands and assignments for chitosan and gelatin.

Bands (cm^{-1}) [a]	Assignment	Reference
Chitosan		
3500–3215/3293 (3292)	N─H stretching; O─H stretching from the saccharide structure	(Lawrie et al., 2007; Qiao et al., 2017; Sionkowska et al., 2004)

2932/2925 (2869)	─CH_2 asymmetric stretching	(Abuibaid et al., 2020; Sionkowska et al., 2004)
1643/1645/1648 (1650)	Amide I (C═O groups)	(Chen et al., 2020a; Chen, Xie, Tang, & McNally, 2020b; Chiono et al., 2008; Lawrie et al., 2007; Meng et al., 2018; Pereda et al., 2011; Sionkowska et al., 2004)
1638–1575/1594/1589 (1589)	Amide II (N─H bending; C─H stretching); Amino group	(Chen et al., 2020a, b; Chen, Xie, Tang, & McNally, 2021b; Chiono et al., 2008; Lawrie et al., 2007; Meng et al., 2018; Yin et al., 2005)
1414 (1418)	O─H bending vibrations	(Chen et al., 2020a; Chiono et al., 2008; Ebrahimi et al., 2019; Meng et al., 2018; Pereda et al., 2011)
1377/1378 (1375)	-CH_2 bending	(Chen et al., 2021b; Chiono et al., 2008; Ebrahimi et al., 2019; Qiao et al., 2017)
1256 (1259)	Amide III (C─N and N─H vibrations; CH_2 groups)	(Chen et al., 2020a; Chiono et al., 2008; Ebrahimi et al., 2019)
1150 (1150)	Asymmetric C─O─C stretching of the saccharide structure	(Chen et al., 2020a; Chiono et al., 2008; Meng et al., 2018; Pereda et al., 2011)
1028–1022 (1024)	C─O stretching of the saccharide structure	(Chen et al., 2020a, b, 2021b; Chiono et al., 2008; Meng et

		al., 2018)
1190–920 (1060/991/894)	C─N stretching; saccharide structure	(Chen et al., 2020a, b; Lawrie et al., 2007; Meng et al., 2018; Pereda et al., 2011)
Gelatin		
3300–3400/3293 (3291)	Amide-A (N─H); O─H	(Abuibaid et al., 2020; Haghighi et al., 2019; Qiao et al., 2017)
2932/2925 (2921)	Amide-B (─CH_2 asymmetric stretching)	(Abuibaid et al., 2020)
1632/1637 (1630)	Amide I (C═O stretching)	(Abuibaid et al., 2020; Pereda et al., 2011; Qiao et al., 2017; Sionkowska et al., 2004)
1554/1537/1535 (1526)	Amide II (40 % C─N and 60% N─H vibrations)	(Pereda et al., 2011; Qiao et al., 2017; Sionkowska et al., 2004; Yin et al., 2005)
1440 (1446)	O─H	(Ebrahimi et al., 2019)
1200–1240/1233 (1235/1198)	Amide III (C─N and N─H vibrations; CH_2 groups)	(Abuibaid et al., 2020; Ebrahimi et al., 2019; Pereda et al., 2011; Qiao et al., 2017; Sionkowska et al., 2004)

[a] The numbers in the brackets are FTIR band positions observed in this current study.

Compared with raw chitosan, the processed chitosan film (100CS) displayed the vibrational bands of amide I and amide III shifting to lower wavenumbers (from 1650 and 1259 cm^{-1} to 1638 and 1257 cm^{-1}) and the vibrational bands of the saccharide structure shifting to higher wavenumbers

(from 1060 and 1024 cm^{-1} to 1068 and 1027 cm^{-1}). These shifts indicate that the original structure of chitosan involving the interactions among these groups was disrupted.

Fig. 2b shows that with the addition of gelatin, the band signals of amide I, II and III for chitosan were increased and there was also slight red shifting of the chitosan adsorption bands (1636, 1547 and 1408 cm^{-1}) to lower wavenumbers (1632, 1543, and 1404 cm^{-1}), which indicates the formation of intermolecular hydrogen bonds between gelatin and chitosan. Meanwhile, the signal of carbohydrate ring skeleton (1150, 1068, and 1027 cm^{-1}) of 25CS decreased and had a blue shift compared to 100CS. However, Lawrie et al. indicated that interaction with ionic species did not cause significant change in the band positions that reflect the carbonyl vibration in alginate (Lawrie et al., 2007).

3.4 Crystalline structure

Fig. 3 shows the XRD patterns for the raw materials and the different chitosan:gelatin films. The diffraction pattern for the raw gelatin displayed a diffuse halo centered on 2θ = 24°, reflecting the random coiled conformation of the macromolecules (Qiao et al., 2017). The diffraction peaks for the raw chitosan at around 2θ = 12° (0 2 0 reflection) and 21° (1 0 0 reflection) can be assigned to its hydrated crystal and regular lattice, respectively (Kittur et al., 2003). Resulting from processing and conditioning, the chitosan film displayed a broad amorphous halo centered around 23° 2θ while the characteristic peaks at 12° 2θ and 21° 2θ of chitosan became unapparent, indicating a predominantly amorphous structure. Some new but weak peaks were observable, which could be due to the formation of new chitosan crystals during conditioning (Chen et al., 2020a). Compared with the 100CS group of films, the composite films were shown to be more amorphous, indicating that gelatin

assisted the processing of chitosan and may also hinder the recrystallization of chitosan during conditioning. This well corresponds to the SEM observation of well-processed chitosan:gelatin samples.

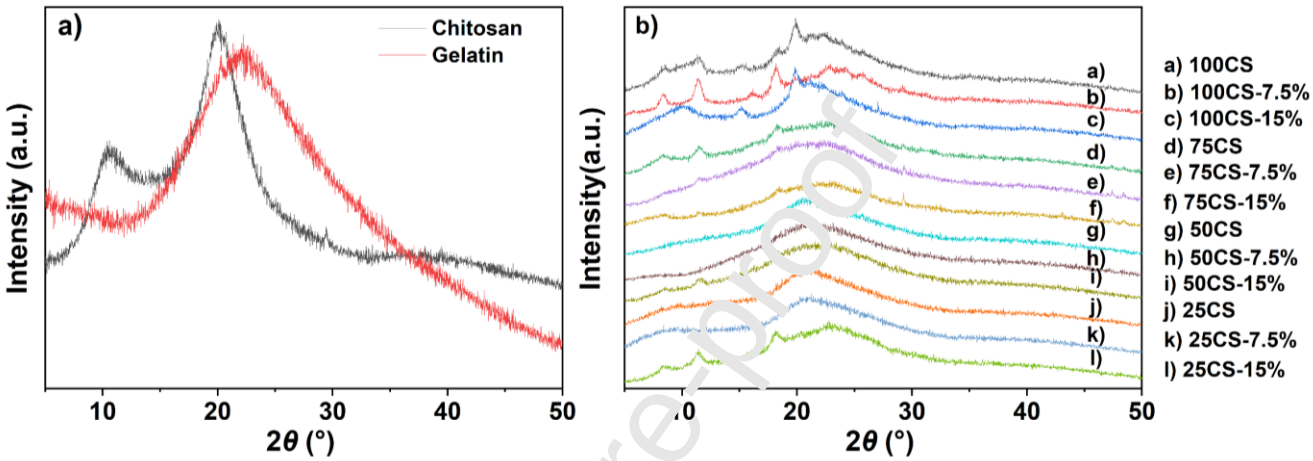

Fig. 3. X-ray diffractograms for a) raw chitosan, raw gelatin, and b) the different chitosan:gelatin films.

3.5 Relaxation temperatures

DMTA was used to obtain the loss tangent (tan δ) profiles as a function of temperature for the different chitosan:gelatin films (**Fig. 4**). All samples exhibited similar tan δ profiles with two obvious transitions identified. The weak transition at this lower temperature region from −50 °C to 0 °C is due to the secondary relaxation (β relaxation) attributed to the motions of side chains or lateral groups of chitosan interacting with small molecules such as water and/or glycerol by hydrogen bonding. A more prominent transition at a higher temperature corresponds to the α relaxation, which can be linked to the glass transition temperature (T_g) of the polymers (Chen et al., 2020a). It can be

seen that 100CS-15% exhibited a significantly lower T_g value than 100CS, indicating increased chain mobility of chitosan due to the plasticization by glycerol. Besides, with increasing gelatin content, T_g first increased and then decreased, with 50CS displayed the highest T_g values (116 ℃ for 50CS-RH57%). Regarding this, a certain amount of gelatin in the system could restrict the mobility of chitosan chains through electrostatic and hydrogen-bonding interactions to the greatest extent. Compared with 57% RH, the samples conditioned at 75% RH showed lower T_g, which can be attributed to the water-induced plasticization effect and decreased intermolecular forces between chitosan and gelatin chains. Irrespective of formulation and RH, the T_g values of all the samples were above room temperature, indicating that they were in a glassy state.

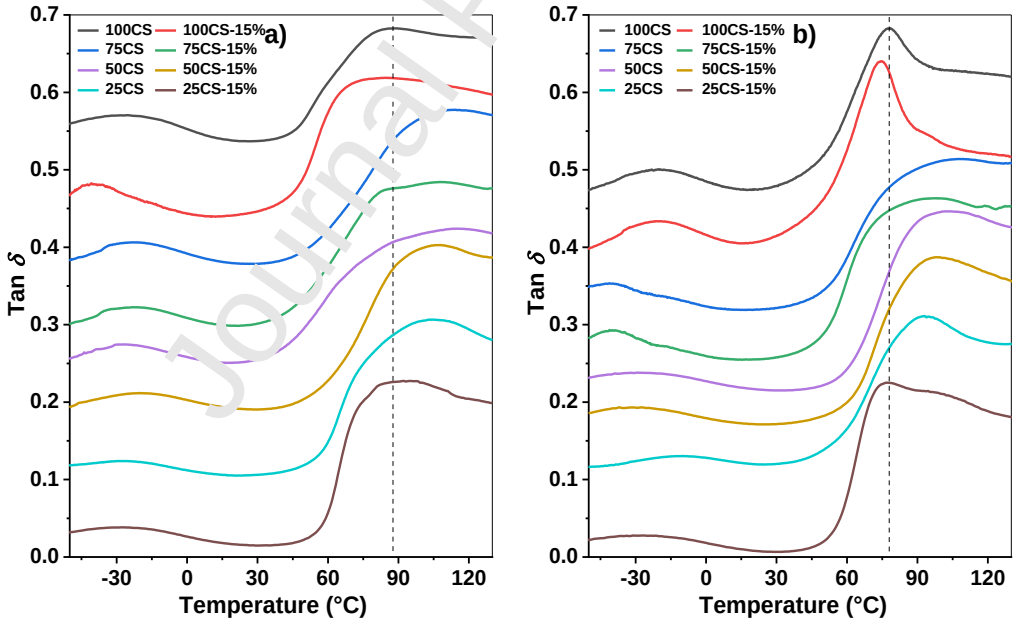

Fig. 4. DMTA curves for the different chitosan:gelatin films in a) RH 75% and b) RH 57%.

3.6 Mechanical properties

Fig. 5 shows the mechanical properties of the chitosan:gelatin films conditioned at 57% RH and 75% RH. From the stress–strain curves (**Fig. 5a** and **Fig. 5e**), we can see the sample 100CS-15% conditioned at 75% RH was the most elastomeric. Other samples conditioned at 75% RH were stiffer. The 50CS film was the stiffest and showed the most apparent strain-hardening behavior, which could be due to the strong interactions between the two biopolymers. **Fig. 5**b-d shows that the 100CS group had the lowest values of Young's modulus (100CS-15%, 22.6 MPa) and tensile strength (100CS-15%, 9.0 MPa), while the 50CS group showed the highest (50CS, 605.3 MPa and 33.6 MPa, respectively). For each chitosan/gelatin ratio, addition of glycerol decreased the Young's modulus and tensile strength while increased the elongation at break, due to the plasticization effect. In particular, the 50CS film showed the lowest elongation at break (32.8%). Among samples conditioned at 75% RH, the 50CS group of films had the best mechanical properties, which could be due to the interactions between chitosan and gelatin.

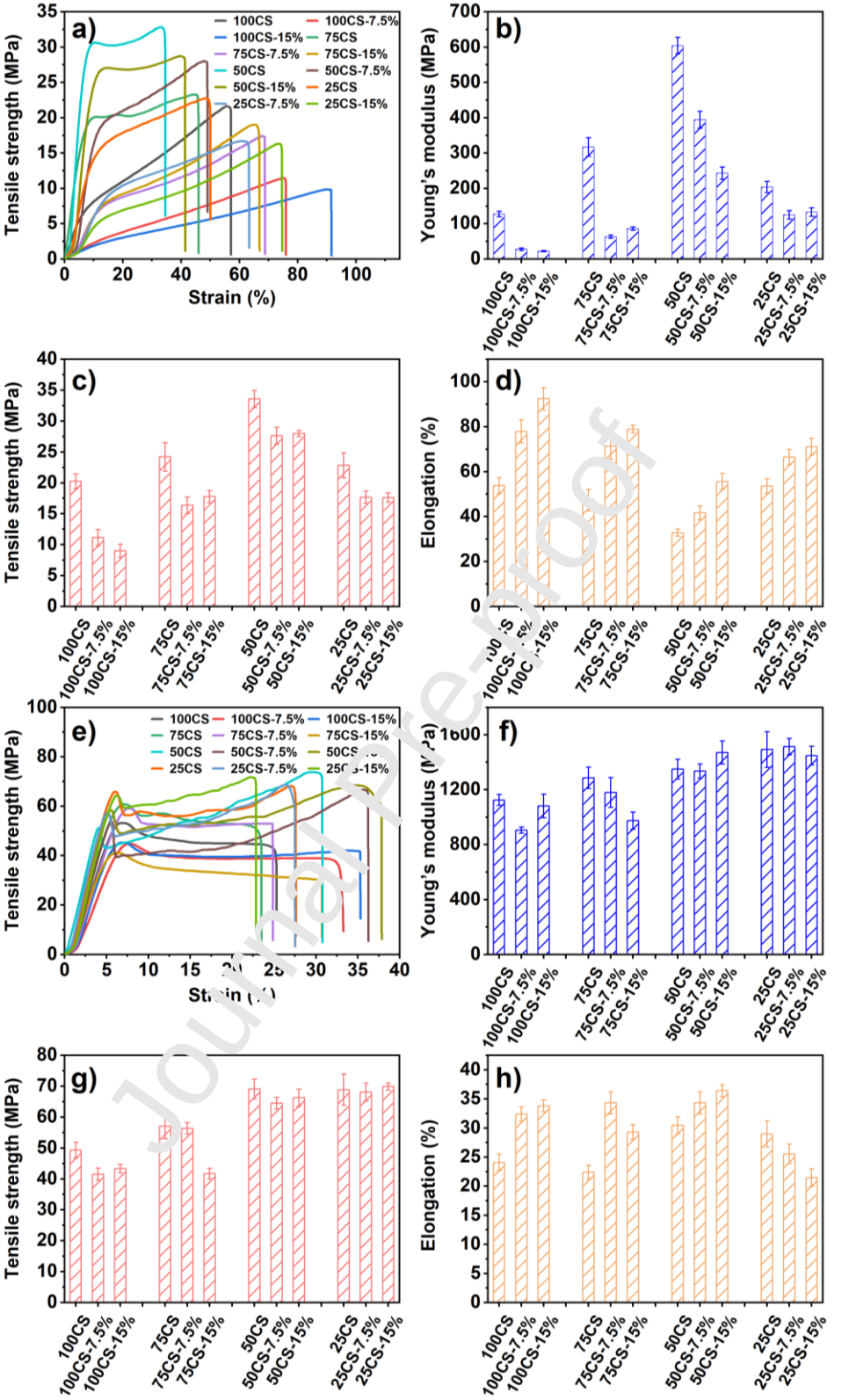

Fig. 5. Mechanical properties of the chitosan:gelatin films conditioned at RH 75% (a–d) and at RH 57% (e–h)

The samples conditioned at RH 57% (**Fig. 5**e-h) were stiffer and more rigid due to a less amount of water molecules in the biopolymers for a plasticization effect, which is as expected. Among these samples, the 50CS and 25CS groups displayed the highest Young's modulus and tensile strength. In this regard, gelatin became more rigid with a lower moisture content, which also contributes to the mechanical properties of the composite system.

3.7 Thermal stability

Fig. 6 shows the TGA results for the raw gelatin, the raw chitosan, and the different chitosan:gelatin films. For the raw chitosan, there was a major thermal decomposition peak between about 200 °C and 400 °C with the peak temperature (T_d) being 303 °C, where the maximum decomposition rate occurred. This result for chitosan agrees with previous reports (Chen et al., 2020a, 2021b; Meng et al., 2018). For the raw gelatin, thermal decomposition occurred mainly between 200 °C and 500 °C with T_d = 326 °C. The thermal decomposition of glycerol started at about 120 °C and ending at 233 °C immediately after the peak temperature.

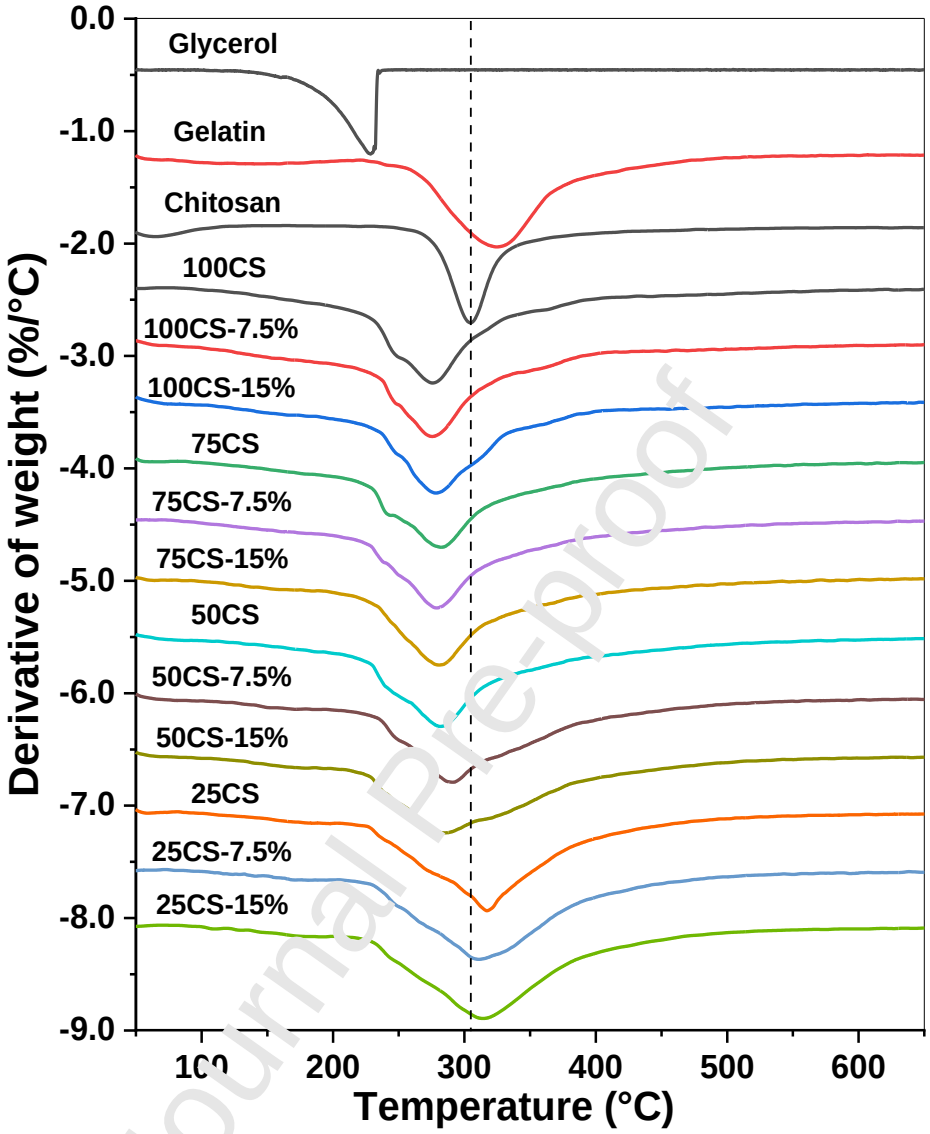

Fig. 6. Derivative TGA curves for the raw chitosan, the raw gelatin, and the different chitosan:gelatin films. The reference line marks the peak temperature of the raw chitosan.

The 100CS film displayed one major thermal decomposition peak with T_d = 275 °C, about 28 °C lower than that of raw chitosan. Besides, there was a small peak at about 250 °C which might be attributed to the initial depolymerization of chitosan. The decreased thermal stability of 100CS could be ascribed to the reduced molecular mass and lower crystallinity resulting from processing.

Compared with 100CS, the composite samples containing gelatin displayed slightly higher T_d, which could be associated with higher thermal stability of the processed gelatin. In other words, the thermal stability of gelatin was less affected by processing than that of chitosan. For the composite films, the addition of glycerol did not change the thermal stability significantly.

3.8 Water absorption and surface hydrophilicity

Fig. 7a shows that all the samples experienced an initial rapid increase in weight during the first 40 min of water soaking and after that point, water absorption continued at a much slower rate. The maximum value of water uptake followed the sequence of 100CS group > 75CS group > 25CS group > 50CS group. After 6 h of water soaking, the 100CS film absorbed water more than 200% as much as its original weight, while the 50CS film had water absorption of about 45%. The lowest water absorption percentage of the 50CS film could be accounted for by the intermolecular interaction between gelatin and chitosan, although each biopolymer was more hygroscopic. A recent study suggested that chitosan:carboxymetnyl cellulose films were more hydrolytically stable than each of the biopolymer component, which was ascribed to the polyelectrolyte complexation between the two biopolymers, stabilizing the chain network structure in water (Chen et al., 2020a). For the reduced water absorption of the 50CS film here, we similarly consider that the electrostatic interactions between chitosan and gelatin led to complexed points for the chain network, which decreased the water swellability and water absorption of the materials. Regarding the higher water absorption of 50CS-7.5% and 50CS-15%, it is proposed that glycerol weakened the electrostatic interaction between chitosan and gelatin.

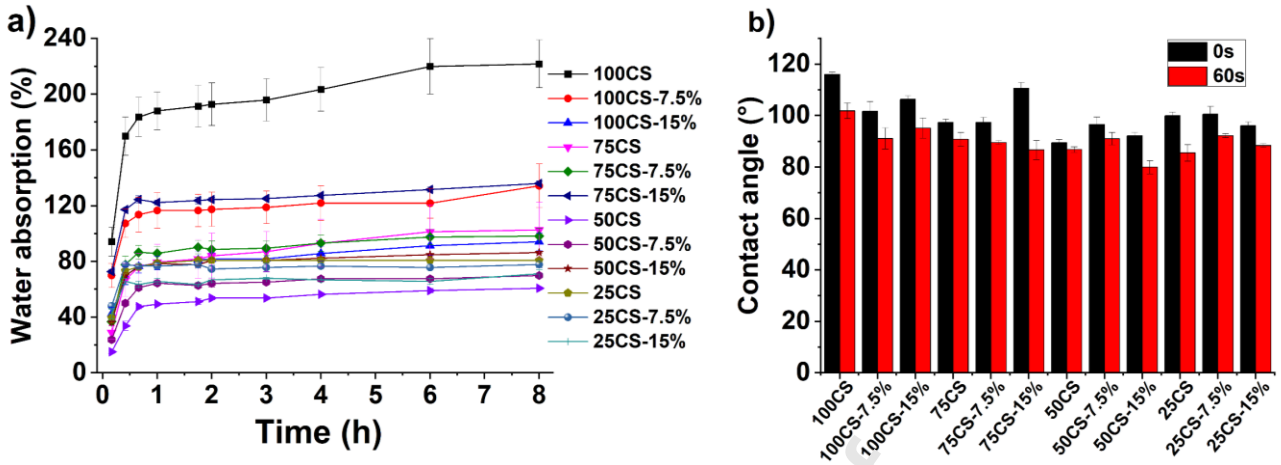

Fig. 7. a) Water absorption percentage of the different biopolymer films; b) Water contact angle measured at 0 s and 60 s for the different chitosan:gelatin films.

Fig. 7b shows the water contact angle (WCA) results of the different chitosan:gelatin films. A higher contact angle means higher surface hydrophilicity, which is largely determined by the surface free energy linked to the chemical groups exposed on the material surface (Chen et al., 2021b). Since a water drop on the films greatly changed with time, WCA was measured at 0 s and 60 s. All the composite films displayed similar WCA values at 0 s (92–115°) and at 60 s (82–101°). Regarding the reduced WCA with time, during wetting, water could disrupt biopolymer chain interactions on the material surface, leading to more free polar groups available to bind water (Chen, Xie, Tang, & McNally, 2021a; Chen et al., 2021b). Among the biopolymer films, the 50CS group had the lowest WCA values, indicating higher surface hydrophilicity. For biopolymers such as gelatin, the high chain mobility would allow for the burying of polar groups in the bulk phase, making the surface more hydrophobic (Yasuda, Sharma, & Yasuda, 1981). Thus, we propose that the intermolecular interaction between the two biopolymers in the 50CS composites could reduce the freedom of the

biopolymers to rearrange themselves to change the material surface configuration. As a result, the 50CS group of films had more polar groups exposed on the material surface and thus, higher surface energy. Moreover, the surface hydrophobicity was reduced with an increasing amount of glycerol, which could be linked to the high hydrophilicity of this plasticizer.

4 Conclusion

In summary, we prepared chitosan:gelatin films by a cost-effective thermomechanical method. We found the properties of chitosan:gelatin films were strongly affected by the chitosan/gelatin ratio, glycerol content, and the conditioning RH. We found a certain ratio of chitosan to gelatin (i.e. the 50CS group of films) led to the lowest water uptake, best mechanically properties, and the highest T_g values. This property enhancement could be ascribed to the strong interactions (e.g. ionic and hydrogen-bonding) between the polysaccharide and the protein as proved by FTIR analysis.

Despite the significantly reduced hygroscopicity of the 50CS group, these formulations displayed the highest surface hydrophilicity, which could be due to the reduced material surface configuration allowing more polar groups exposed on the material surface. This contrast shows the surface hydrophilicity and overall hygroscopicity are controlled by different mechanisms for biopolymer materials. Besides, addition of gelatin made chitosan more amorphous, which could be due to the restriction of chitosan chain rearrangement by gelatin. While the pure chitosan films were the darkest and most opaque, composite films with a higher content of gelatin were brighter and more transparent, and thus better visual appearance. Glycerol, as a plasticizer, assisted the processing of chitosan as shown by SEM, and gelatin was found to have a similar effect.

Thus, this study could be insightful for the design of cost-effective biopolymer materials with

tailored properties for specific applications (e.g. packaging, coating, and biomedical).

Acknowledgement

This work was supported by the National Key Research and Development Program of China (2018YFD0400702), the Guangdong Province Key-Area R&D program (2019B020210002), and the 111 Project (B17018). Y. Chen acknowledges the State Scholarship Fund provided by the China Scholarship Council (CSC) for supporting her studies at the National University of Singapore.

Declaration of interests

None.

References

Abuibaid, A., AlSenaani, A., Hamed, F., Kittiphattanabawon, P., & Maqsood, S. (2020). Microstructural, rheological, gel-forming and interfacial properties of camel skin gelatin. *Food Structure, 26*, Article 100156.

Alexandre, E. M. C., Lourenço, R. V., Bittante, A. M. Q. B., Moraes, I. C. F., & Sobral, P. J. d. A. (2016). Gelatin-based films reinforced with montmorillonite and activated with nanoemulsion of ginger essential oil for food packaging applications. *Food Packaging and Shelf Life, 10*, 87-96.

An, J., Gou, Y., Yang, C., Hu, F., & Wang, C. (2013). Synthesis of a biocompatible gelatin functionalized graphene nanosheets and its application for drug delivery. *Materials Science and Engineering C, 33*(5), 2827-2837.

Aramesh, N., Bagheri, A. R., & Bilal, M. (2021). Chitosan-based hybrid materials for adsorptive

removal of dyes and underlying interaction mechanisms. *International Journal of Biological Macromolecules, 183*, 399-422.

Astaneh, M. E., Goodarzi, A., Khanmohammadi, M., Shokati, A., Mohandesnezhad, S., Ataollahi, M. R., et al. (2020). Chitosan/gelatin hydrogel and endometrial stem cells with subsequent atorvastatin injection impact in regenerating spinal cord tissue. *Journal of Drug Delivery Science and Technology, 58*, Article 101831.

Avena-Bustillos, R. J., Cisneros-Zevallos, L. A., Krochta, J. M., & Saltveit, M. E. (1994). Application of casein-lipid edible film emulsions to reduce white blush on minimally processed carrots. *Postharvest Biology and Technology, 4*(4), 319-329.

Boekel, V. M. A. J. S. (1996). Statistical Aspects of Kinetic Modeling for Food Science Problems. *J Food Sci, 61*(3), 477-486.

Chen, P., Xie, F., Tang, F., & McNally, T. (2020a). Thermomechanical-induced polyelectrolyte complexation between chitosan and carboxymethyl cellulose enabling unexpected hydrolytic stability. *Composites Science and Technology, 189*, Article 108031.

Chen, P., Xie, F., Tang, F., & McNally, T. (2020b). Structure and properties of thermomechanically processed chitosan/carboxymethyl cellulose/graphene oxide polyelectrolyte complexed bionanocomposites. *International Journal of Biological Macromolecules, 158*, 420-429.

Chen, P., Xie, F., Tang, F., & McNally, T. (2021a). Cooperative Effects of Cellulose Nanocrystals and Sepiolite When Combined on Ionic Liquid Plasticised Chitosan Materials. *Polymers, 13*, Article 571.

Chen, P., Xie, F., Tang, F., & McNally, T. (2021b). Influence of plasticiser type and nanoclay on the

properties of chitosan-based materials. *European Polymer Journal, 144*, Article 110225.

Chiono, V., Pulieri, E., Vozzi, G., Ciardelli, G., Ahluwalia, A., & Giusti, P. (2008). Genipin-crosslinked chitosan/gelatin blends for biomedical applications. *Journal of Materials Science: Materials in Medicine, 19*, 889-898.

Ebrahimi, S., Fathi, M., & Kadivar, M. (2019). Production and characterization of chitosan-gelatin nanofibers by nozzle-less electrospinning and their application to enhance edible film's properties. *Food Packaging and Shelf Life, 22*, Article 100387

Epure, V., Griffon, M., Pollet, E., & Avérous, L. (2011). Structure and properties of glycerol-plasticized chitosan obtained by mechanical kneading. *Carbohydrate Polymers, 83*(2), 947-952.

Guo, J., Li, X., Mu, C., Zhang, H., Qin, P., & Li, D. (2013). Freezing–thawing effects on the properties of dialdehyde carboxymethyl cellulose crosslinked gelatin-MMT composite films. *Food Hydrocolloids, 33*(2), 273-279.

Haghighi, H., De Leo, R., Bedin, E., Pfeifer, F., Siesler, H. W., & Pulvirenti, A. (2019). Comparative analysis of blend and bilayer films based on chitosan and gelatin enriched with LAE (lauroyl arginate ethyl) with antimicrobial activity for food packaging applications. *Food Packaging and Shelf Life, 19*, 31-39.

Ji, Z., Liu, H., Yu, L., Duan, Q., Chen, Y., & Chen, L. (2020). pH controlled gelation behavior and morphology of gelatin/hydroxypropylmethylcellulose blend in aqueous solution. *Food Hydrocolloids, 104*, Article 105733.

Kittur, F. S., Vishu Kumar, A. B., & Tharanathan, R. N. (2003). Low molecular weight

chitosans—preparation by depolymerization with Aspergillus niger pectinase, and characterization. *Carbohydrate Research, 338*(12), 1283-1290.

Kurakula, M., Gorityala, S., & Moharir, K. (2021). Recent Trends in Design and Evaluation of Chitosan-based Colon Targeted Drug Delivery Systems: Update 2020. *Journal of Drug Delivery Science and Technology, 64*, Article 102579.

Lawrie, G., Keen, I., Drew, B., Chandler-Temple, A., Rintoul, L., Fredericks, P., et al. (2007). Interactions between Alginate and Chitosan Biopolymers Characterized Using FTIR and XPS. *Biomacromolecules, 8*, 2533-2542.

Li, X., Xing, R., Xu, C., Liu, S., Qin, Y., Li, K., et al. (2021). Immunostimulatory effect of chitosan and quaternary chitosan: A review of potential vaccine adjuvants. *Carbohydrate Polymers, 264*, Article 118050.

Meng, L., Xie, F., Zhang, B., Wang, D. K., & Yu, L. (2018). Natural Biopolymer Alloys with Superior Mechanical Properties. *ACS Sustainable Chemistry & Engineering, 7*(2), 2792-2802.

Nur Hanani, Z. A., Roos, Y. H., & Kerry, J. P. (2014). Use and application of gelatin as potential biodegradable packaging materials for food products. *International Journal of Biological Macromolecules, 71*, 94-102.

Pereda, M., Ponce, A. G., Marcovich, N. E., Ruseckaite, R. A., & Martucci, J. F. (2011). Chitosan-gelatin composites and bi-layer films with potential antimicrobial activity. *Food Hydrocolloids, 25*(5), 1372-1381.

Qiao, C., Ma, X., Zhang, J., & Yao, J. (2017). Molecular interactions in gelatin/chitosan composite

films. *Food Chemistry, 235*, 45-50.

Rivero, S., García, M. A., & Pinotti, A. (2009). Composite and bi-layer films based on gelatin and chitosan. *Journal of Food Engineering, 90*(4), 531-539.

Rodrigues, M. A. V., Bertolo, M. R. V., Marangon, C. A., Martins, V., & Plepis, A. M. G. (2020). Chitosan and gelatin materials incorporated with phenolic extracts of grape seed and jabuticaba peel: Rheological, physicochemical, antioxidant, antimicrobial and barrier properties. *International Journal of Biological Macromolecules, 160*, 769-779.

Roy, S., & Rhim, J.-W. (2020). Preparation of antimicrobial and antioxidant gelatin/curcumin composite films for active food packaging application. *Colloids and Surfaces B: Biointerfaces, 188*, Article 110761.

Sionkowska, A., Wisniewskia, M., Skopinskaa, J., Kennedy, C. J., & Wess, T. J. (2004). Molecular interactions in collagen and chitosan blends. *Biomaterials, 25*(5), 795-801.

Sun, J., Huang, Y., Wang, W., Yu, Z., Wang, A., & Yuan, K. (2008). Application of gelatin as a binder for the sulfur cathode in lithium–sulfur batteries. *Electrochimica Acta, 53*(24), 7084-7088.

Torkaman, S., Rahmani, H., Ashori, A., & Najafi, S. H. M. (2021). Modification of chitosan using amino acids for wound healing purposes: A review. *Carbohydrate Polymers, 258*, Article 117675.

Wang, H., Ding, F., Ma, L., & Zhang, Y. (2021). Edible films from chitosan-gelatin: Physical properties and food packaging application. *Food Bioscience, 40*, Article 100871.

Wu, S., Dong, H., Li, Q., Wang, G., & Cao, X. (2017). High strength, biocompatible hydrogels with designable shapes and special hollow-formed character using chitosan and gelatin.

Carbohydrate Polymers, 168, 147-152.

Xu, J., Wei, R., Jia, Z., & Song, R. (2020). Characteristics and bioactive functions of chitosan/gelatin-based film incorporated with ε-polylysine and astaxanthin extracts derived from by-products of shrimp (Litopenaeus vannamei). *Food Hydrocolloids, 100*, Article 105436.

Yang, D., Li, Y., & Nie, J. (2007). Preparation of gelatin/PVA nanofibers and their potential application in controlled release of drugs. *Carbohydrate Polymers, 69*(3), 538-543.

Yasuda, H., Sharma, A. K., & Yasuda, T. (1981). Effect of orientation and mobility of polymer molecules at surfaces on contact angle and its hysteresis. *Journal of Polymer Science: Polymer Physics Edition, 19*(9), 1285-1291.

Yin, Y., Li, Z., Sun, Y., & Yao, K. (2005). A preliminary study on chitosan/gelatin polyelectrolyte complex formation. *Journal of materials science, 40*(17), 4649-4652.

Zhang, H., Liang, Y., Li, X., & Kang, H. (2020). Effect of chitosan-gelatin coating containing nano-encapsulated tarragon essential oil on the preservation of pork slices. *Meat science, 166*, Article 108137.

Zhang, Y., Zhao, M., Cheng, Q., Wang, C., Li, H., Han, X., et al. (2021). Research progress of adsorption and removal of heavy metals by chitosan and its derivatives: A review. *Chemosphere, 279*, Article 130927.

Zhao, J., Wei, F., Xu, W., & Han, X. (2020). Enhanced antibacterial performance of gelatin/chitosan film containing capsaicin loaded MOFs for food packaging. *Applied Surface Science, 510*, Article 145418.

CRediT author statement:

Ying Chen: Methodology, Validation, Formal analysis, Investigation, Data Curation, Writing - Original Draft, Visualization. **Qingfei Duan**: Validation, Formal analysis, Investigation, Data Curation, Visualization. **Long Yu:** Resources, Project administration, Funding acquisition. **Fengwei Xie**: Conceptualization, Methodology, Resources, Writing - Review & Editing, Visualization, Supervision.

Graphical abstract

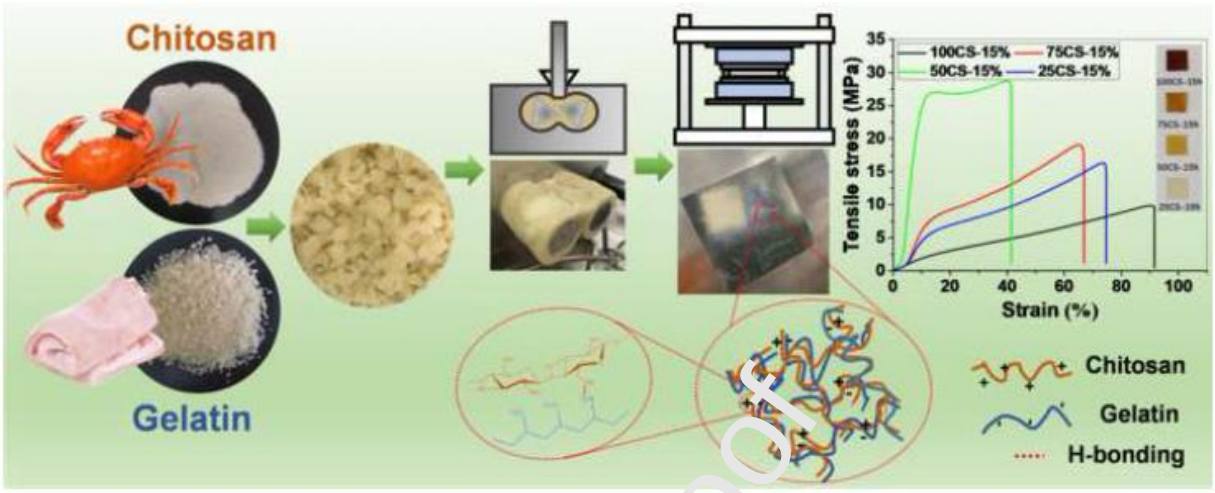

Highlights:

- ✓ Chitosan:gelatin composite materials processed by high-viscosity thermo-mixing
- ✓ Biopolymer material properties controlled by formulation and relative humidity
- ✓ 1:1 Chitosan:gelatin had the best mechanical properties and lowest hygroscopicity
- ✓ 1:1 Chitosan:gelatin film showed the highest surface hydrophilicity
- ✓ Chitosan added with gelatin had improved processibility and higher transparency